ELSEVIER

Journal of Photochemistry and Photobiology A: Chemistry 149 (2002) 227–236

Journal of Photochemistry and Photobiology A:Chemistry

www.elsevier.com/locate/jphotochem

Short communication

Photo-physics of surface-treated titanium dioxides

Michael Schiller [a,*], Franz Werner Müller [b], Cornelia Damm [b]

[a] *Chemson Polymer-Additive AG, Industriestr. 19, A-9601 Arnoldstein, Austria*

[b] *Martin-Luther-University Halle-Wittenberg, Institute of Organic Chemistry, Geusaer Str. 46, D-06217 Merseburg, Germany*

Received 20 December 2001; accepted 7 January 2002

Abstract

The photoelectric properties of commercially used TiO_2 pigments were studied by transient photo-electromotive-force (PEMF) measurements. The influence of the crystal structure (anatase or rutile) and the pigment coating (and other) on the PEMF parameters of TiO_2 was investigated. Pure anatase type pigments show in the microsecond time range a creation of a positive PEMF signal. In the millisecond time range the PEMF decay starts with a positive sign. This means that anatase pigments behave as typical n-type photoconductors. However, pure rutile type pigments show in the microsecond time range a negative PEMF signal or a signal starting with negative sign. This means that rutile pigments act as typical p-type photoconductors during the first few microseconds. Coating of rutile or anatase pigments decrease the PEMF maximum voltages U_{max} in comparison to untreated pigments. However, in some cases coating creates an increase of the PEMF decay rate which is explained by an increase of the charge carrier recombination. Rutile pigments epitaxially coated with Al_2O_3 and SiO_2 may show very complex PEMF signals with two negative maximum voltages. Such types of signals may indicate heterojunctions between the TiO_2 core and the coating shell. In this way the PEMF parameters are an excellent tool to characterise TiO_2 pigments. © 2002 Published by Elsevier Science B.V.

Keywords: TiO_2; Photo-electromotive-force (PEMF); Surface treatment; Coating

1. Introduction

TiO_2 pigments are widely used as fillers and light shielding substances in polymer materials. However, TiO_2 may be a photocatalytic active pigment [1–5] also. So the TiO_2 pigment may contribute to the degradation of surrounding polymer material under illumination by sunlight. In most cases this effect is unwanted because it decreases the weathering stability of the material. For that reason the surface of the pigments is treated.

The long-term weathering of white PVC-profiles has been intensively investigated and published. Theoretical mechanisms have been proposed and are supported by experiments in model systems. Nonetheless, there are a number of colour-like changes that cause problems for profile manufacturers. From our own experience and from the literature [6–10] photo-effects within short irradiation times (between 2 and 200 h) are known. For example, photoblueing, in which the profile becomes lighter, is not unknown in Europe. Schiller [11] proposed the mechanism shown in Fig. 1.

Notwithstanding the different and partial contradictory mechanisms, the first step of photo-degradation is always light absorption by the TiO_2. It is connected with generation and separation of charge carriers in the pigment. That is the decisive step of all further processes on the pathway of photo-degradation which follow in the dark. Therefore the characterisation of the photoelectric properties of pigments may be the key to estimate their photo-degradative potential in the polymer matrix. Time resolved photo-electromotive-force (PEMF) measurements reflect these properties.

Light irradiation promotes electrons (e^-) from the valence band (VB) into the conduction band (CB) of the photoconductor TiO_2. These electrons leave positive holes (h^+) at the VB. Electrons as well as holes can trigger a number of photocatalytic processes starting on the pigment surface; see Fig. 1. Electron transfer to oxygen (a) probably plays an inferior role in these investigations, but it generates hydrogen peroxide or alkylhydroperoxides. Hydroxy- or alkoxy-radicals ($RO^\bullet$/$HO^\bullet$) can be formed by electron transfer to hydroperoxides like ROOH or HOOH (b). In the case of PVC a photoinduced cleavage of the C–Cl bond (c) may also be considered. In this way carbon radicals are generated

* Corresponding author. Tel.: +43-4255-2226-0; fax: +43-4255-2435.
E-mail address: michael.schiller@chemson.com (M. Schiller).

1010-6030/02/$ – see front matter © 2002 Published by Elsevier Science B.V.
PII: S1010-6030(02)00009-6

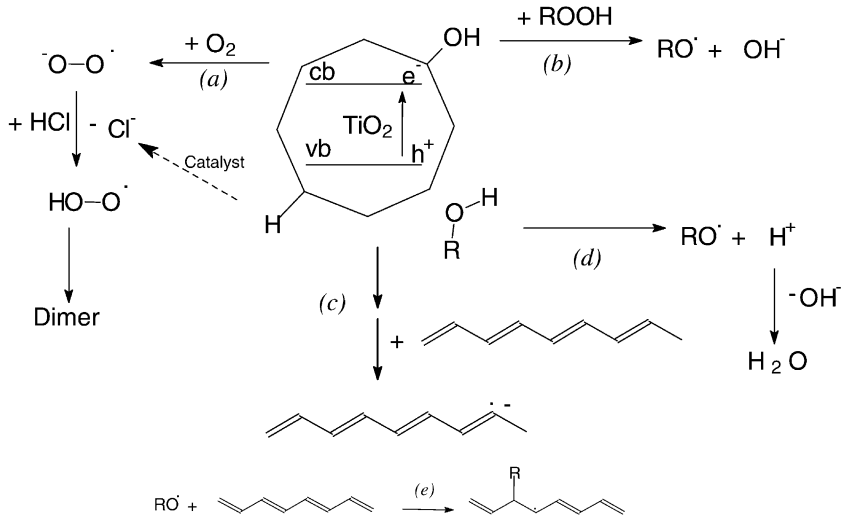

Fig. 1. Suggested mechanisms of photo-redox processes on TiO_2 (a–d) in relation to photoblueing of PVC (e) [11].

which are a new source for peroxy radicals and peroxides in the presence of oxygen. Radical cations and radicals may also be generated by a hole (h^+) transfer to electron donors or nucleophiles like alcohols and polyols (used as co-stabiliser) (d). Their reaction with the polyene chain of partially decomposed PVC (e) may interrupt the conjugation in the π-system which gives a yellowish colour to the white profile. The onlooker sees this as a "blueing effect", but in actual fact it may best be described as a "less yellowing effect". To estimate their photocatalytic activity we have investigated the photoelectric properties of several simple and surface-treated titanium dioxides by laser PEMF technique.

2. Description of the method

The PEMF parameters sign, maximum value (U_{max}) and decay behaviour (rate constant k) characterise any photoconductor. Fig. 2 shows the principle of PEMF generation. The gradient of light absorption creates a charge carrier concentration gradient which is the driving force of the charge carrier diffusion into the bulk. If electrons and holes have different mobilities, a spatial charge separation takes place. An internal electric field arises between the illuminated and the dark side of the sample. This field can be measured as an electric potential difference—the PEMF.

PEMF measurements were carried out without contact and without any external electric field. So charge carrier concentration gradient and/or internal space charges are the sole driving forces for PEMF generation. This means that this method does measure the natural behaviour of charge carriers. Changes in the structure of the sample cause changes in the PEMF parameters. The type of photoconduction determines the sign of PEMF. In the PEMF device used in our experiments, n-type photoconductors like TiO_2 show PEMF signals which are positive. The maximum PEMF (U_{max}) represents the maximum potential within the time dependence of the PEMF. U_{max} increases with increasing number of charge carriers generated by the laser flash. So the amount of U_{max} could be one relative measure for the photocatalytic activity of a given pigment.

The separated charge carriers can initiate charge transfer reactions with the resin and its ingredients and cause chemical processes within the surrounding material (heterogeneous photocatalysis). This and the charge carrier annihilation by recombination cause a decay of the PEMF (rate constant k).

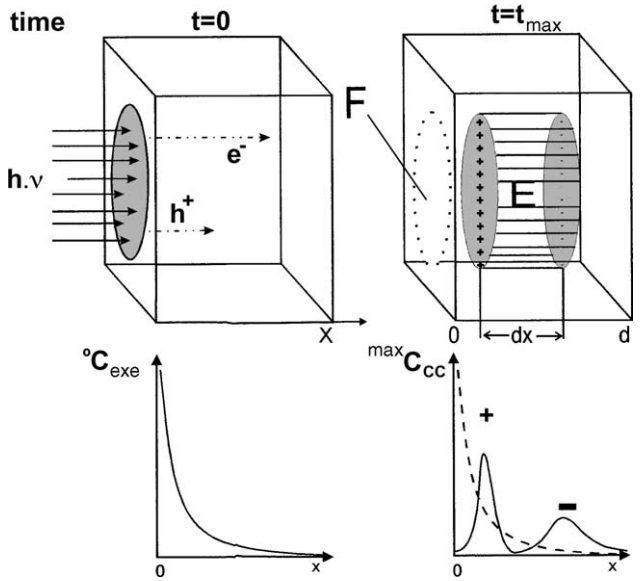

Fig. 2. Principle of the PEMF generation in a single crystal. ${}^0C_{exc}$: charge carrier distribution at zero time $t = 0$; ${}^{max}C_{CC}$: charge carrier distribution at $t = t_{max}$ if the PEMF $U = U_{max}$; F: illuminated area; E: internal electric field at $t = t_{max}$; d: thickness of the sample, dx: distance of the centres of charges at $t = t_{max}$.

In this work the kinetics of the PEMF signals was evaluated (as far as possible) by using a biexponential model; Eq. (1) [12,13]. According to Eqs. (2) and (3) the experimental values of both partial PEMFs U_1^0 and U_2^0 were related to the maximum value of the PEMF U_{max}.

$$U(t) = U_1^0 \exp(-k_1 t) + U_2^0 \exp(-k_2 t) \quad (1)$$

$$U_{max} = U_1^0 + U_2^0 \quad (2)$$

$$U_{2,norm}^0 = \frac{U_{max}}{(1 + U_{1,exp}^0 / U_{2,exp}^0)} \quad (3)$$

In the kinetics U_1^0 represents the potential of the subsurface and U_2^0 the potential of the bulk in the pigment grains. k_1 and k_2 represent the rate constants of the recombination in the subsurface and in the bulk [12,13]. Its reciprocals can be interpreted as the lifetime of charge carriers. The photocatalytic activity of a pigment should increase with increasing $1/k$ because the charge carriers are available for a longer time. The ratios of k_1/k_2 and U_1^0/U_2^0 show the difference of the charge carrier behaviour at the subsurface and the bulk regions of a given photoconductor. The amount of the quotient increases with increasing difference in the behaviour of both regions. A negative sign in the relation U_1^0/U_2^0 indicates that the PEMF crosses the zero potential during its decay process.

3. Experimental

3.1. Investigated TiO_2 pigments

The TiO_2 pigments investigated were purchased from "Kronos". The investigated titanium dioxides are characterised in Table 1.

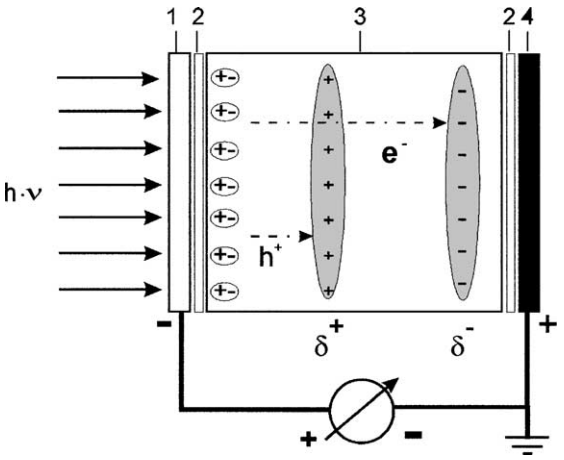

Fig. 3. Principle of PEMF measurement: (1) transparent NESA glass electrode; (2) insulating foils; (3) sample; (4) metal electrode.

3.2. Sample preparation

One hundred milligrams of the pigment was dispersed by ultrasonics in 3 g of a 10% solution of polyvinyl butyrale in 1,2-dichloroethane. The mixture was placed on a glass plate (27 cm^2 in area). After drying the pigment, the polymer layer was removed from the glass support. The remaining solvent was removed under vacuum. The resulting pigment polymer layers have a thickness of about 100 μm and total absorbency in the UV.

3.3. PEMF measurements

Fig. 3 shows the principle of PEMF measurement. The cell for PEMF measurements is constructed like a capacitor with

Table 1
Investigated titanium dioxides by Kronos and available data (Type: R = rutile, A = anatase; weathering: 1 = highest, 2 = good, 3 = yes) [14]

Name	Type	Coating			Content (%)	Density (g/ml)	Oil nr. (kg/m^3)	Weathering
		Al	Si	Other				
Kronos 1001	A				99.0	3.8	20	
Kronos 1014	A	+			97.5	3.8	18	
Kronos 1071	A	+	+		96.0	3.7	20	
Kronos 1080	A			Sb	98.0	3.8	20	
Kronos 2044	R	+	+		82.0	3.6	38	2
Kronos 2056	R	+	+		94.0	4.1	20	2
Kronos 2059	R	+			93.5	4.1	19	3
Kronos 2081	R	+	+		91.0	4.0	21	1
Kronos 2084	R	+			93.0	4.0	15	1
Kronos 2087	R	+			87.0	3.8	20	1
Kronos 2160	R	+	+		90.5	3.9	18	1
Kronos 2190	R	+		Zr	94.0	4.1	18	2
Kronos 2220	R	+	+		92.5	4.0	17	1
Kronos 2257	R	+	+		91.0	3.9	24	1
Kronos 2310	R	+	+	Zr	92.5	4.0	16	1
Kronos 2400	R	+			97.0	4.2	13	3
Kronos 3000	A				99.0	3.8		
Kronos 3025	R				99.0	4.2		
WJ 127/99[a]	R				85.0			

[a] Kronos 3025 coated with 15% of a cross-linked silicon-rubber.

the sample as dielectric. The sample is flash-illuminated by a nitrogen laser type "PNL100" (LTB Lasertechnik Berlin, $\lambda_{flash} = 337$ nm, $\tau_{1/2} = 0.3$ ns, 2.7×10^{13} quanta per flash). The resulting PEMF is measured without any galvanic contact because there are insulating foils between sample and electrodes. This prevents charge injection from the electrodes into the sample. The preamplifier has an impedance of about 1 TΩ and the PEMF measurements take place without any external electric field. The maximum time resolution of our device is about 40 ns. All experiments were carried out in air under normal pressure and at 298 K. In all cases the signal of the first laser flash was recorded. After that sampling of four signals was done. For sampling experiments the time distance between two flashes was 120 s. A more detailed description of the used PEMF device is given in literature [12].

4. Results and discussion

The PEMF parameters of the investigated TiO_2 pigments are summarised in Table 2 (up to 2.5 μs) and in Table 3 (up to 200 ms). In most cases no significant difference in the signals was found between single excitation and sampling of four excitations. Exceptions from that will be discussed later.

All titanium dioxides of the anatase-type show in the time range up to 2.5 μs a generation of a positive signal. Furthermore they show in the time range up to 200 ms a PEMF signal with an intercept of the 0-line starting with a positive sign. Hence, the graphs of the anatase-type pigments exhibit the behaviour of a typical n-type photoconductor. Fig. 4a and b show the PEMF signal of "Kronos 3000" as an example for an anatase.

Table 2
Kinetic parameters of PEMF measurements of several titanium dioxides in PVB (time range: 0–2.5 μs); S: only the signal rise could be recorded

Sample	U_{max} (mV)	U_1 (mV)	U_2 (mV)	k_1 ($\times 10^{-6}$ s)[a]	k_2 ($\times 10^{-5}$ s)[a]	U_1/U_2	k_1/k_2
(a) *Signals after the first flash*							
Kronos 1001	S						
Kronos 1014	S						
Kronos 1071	S						
Kronos 1080	S						
Kronos 3000	S						
Kronos 2044	−7.3	−1.0	−6.4	2.0	0.6	0.2	33
Kronos 2056	−18.8	−3.9	−14.9	3.9	1.3	0.3	30
Kronos 2059[a]	−3.0	−2.6	−0.4	94.0	44.0	6.5	21
Kronos 2081	−25.9	−8.1	−17.8	2.8	0.9	0.4	30
Kronos 2084	−26.3	−5.6	−20.6	2.8	0.6	0.3	47
Kronos 2087	−37.6	−5.4	−32.2	3.6	0.5	0.2	77
Kronos 2160	−14.8	−8.6	−6.2	9.5	2.4	1.4	40
Kronos 2190	−4.4	−0.4	−4.0	14.9	9.7	0.1	15
Kronos 2220	−20.5	−15.2	−5.3	12.0	4.7	2.9	26
Kronos 2310	−13.3	−9.2	−4.1	10.2	4.8	2.2	21
Kronos 2400	−9.0	−6.6	−2.4	14.9	6.5	2.8	23
Kronos 3025	−35.4	−16.2	−19.2	6.6	3.4	0.8	19
WJ 127/99	−38.7	−11.0	−27.8	4.9	1.0	0.4	50
(b) *Sampling of four signals in series; time between two flashes*: 120 s							
Kronos 1001	S						
Kronos 1014	S						
Kronos 1071	S						
Kronos 1080	S						
Kronos 3000	S						
Kronos 2044	−7.2	−0.8	−6.4	2.2	0.7	0.1	31
Kronos 2056	−19.3	−3.8	−15.5	3.9	1.3	0.2	30
Kronos 2059[a]	−2.8	−2.6	−0.3	96.0	46.0	8.7	21
Kronos 2081	−25.8	−8.0	−17.8	2.8	1.0	0.4	29
Kronos 2084	−25.8	−5.6	−20.2	2.8	0.6	2.8	46
Kronos 2087	−37.2	−5.6	−31.6	3.5	0.5	0.2	76
Kronos 2160	−14.5	−8.5	−6.0	9.1	2.4	1.4	38
Kronos 2190	−4.6	−0.5	−4.1	12.0	9.3	0.1	13
Kronos 2220	−19.7	−15.0	−4.7	12.0	5.2	3.2	23
Kronos 2310	−13.3	−9.0	−4.2	9.8	4.6	2.1	21
Kronos 2400	−11.1	−6.6	−4.4	11.0	2.2	1.5	50
Kronos 3025	−37.6	−16.3	−21.3	6.2	2.7	0.8	23
WJ 127/99	−42.0	−11.0	−31.0	4.5	0.8	0.4	56

[a] Only one intercept with the 0-line in the considered time range.

Table 3
Kinetic parameters of PEMF measurements of several titanium dioxides in PVB (time range: 0–200 ms)

Sample	U_{max} (mV)	U_1 (mV)	U_2 (mV)	k_1 (s)	k_2 (s)	U_1/U_2	k_1/k_2
(a) *Signals after the first flash*							
Kronos 1001	60.2	418	−412	51	45	−1.0	1.1
Kronos 1014	19.2	255	−253	45	44	−1.0	1.0
Kronos 1071	14.3	163	−162	47	46	−1.0	1.0
Kronos 1080	12.2	1500	−1487	48	47	−1.0	1.0
Kronos 3000	50.7	96	−46	87	37	−2.1	2.4
Kronos 2044	−2.0	−508	506	76	75	−1.0	1.0
Kronos 2056	−4.3	−960	955	45	44	−1.0	1.0
Kronos 2059	7.6	14	−6	69	27	−2.4	2.6
Kronos 2081	−7.1	−1008	1001	50	49	−1.0	1.0
Kronos 2084	−10.0	−247	237	60	43	−1.0	1.4
Kronos 2087	−22.7	−5068	5046	45	44	−1.0	1.0
Kronos 2160	−1.8	−3	1	111	30	−2.8	3.7
Kronos 2190	7.6	12	−4	68	20	−3.1	3.4
Kronos 2220	1.0	252	−250	43	42	−1.0	1.0
Kronos 2310	1.7	166	−164	42	35	−1.0	1.2
Kronos 2400	1.4	302	−301	30	29	−1.0	1.0
Kronos 3025	19.2	25	−6	87	17	−4.3	5.2
WJ 127/99	−6.0	−1580	1574	51	50	−1.0	1.0
(b) *Sampling of four signals in series; time between two flashes*: 120 s							
Kronos 1001	57.7	4162	−4105	52	44	−1.0	1.2
Kronos 1014	16.6	2264	−2247	46	45	−1.0	1.0
Kronos 1071	13.3	832	−819	48	47	−1.0	1.0
Kronos 1080	10.6	1464	−1453	47	46	−1.0	1.0
Kronos 3000	49.8	92	−42	90	37	−2.1	2.4
Kronos 2044	−2.0	−481	479	78	77	−1.0	1.0
Kronos 2056	−3.4	−718	714	47	46	−1.0	1.0
Kronos 2059	7.5	12	−5	71	26	−2.4	2.8
Kronos 2081	−7.7	−1186	1179	51	50	−1.0	1.0
Kronos 2084	−10.5	−74	64	55	46	−1.2	1.2
Kronos 2087	−20.4	−4544	4524	45	44	−1.0	1.0
Kronos 2160	−1.8	−3	1	110	35	−2.8	3.2
Kronos 2190	7.5	12	−5	64	23	−2.4	2.7
Kronos 2220	1.0	129	−127	40	28	−1.0	1.4
Kronos 2310	1.6	165	−163	39	38	−1.0	1.0
Kronos 2400	−1.8	−3	2	145	51	−2.1	2.9
Kronos 3025	16.6	21	−5	87	16	−4.4	5.4
WJ 127/99	−8.0	−2018	2010	50	50	−1.0	1.0

All titanium dioxides of the rutile-type show in a time range up to 2.5 μs a negative signal or a signal starting with negative sign and crossing the zero potential. This seems to be typical for rutiles which behave as p-type photoconductors in the microsecond range. But in the millisecond time range a PEMF signal is observed starting with positive sign. Fig. 5a and b show the PEMF signal of "Kronos 3025" as an example for a rutile pigment.

However, we have not found identical graphs for the different anatase-type pigments or for the different rutile-type pigments, Tables 2 and 3. Therefore, we conclude that the different graphs are caused by the different coatings.

The results shown in Tables 2 and 3 may be summarised as follows:

- The U_{max} values for the Kronos anatase-types (Table 3) are in a range between 10 and 60 mV with the highest value for Kronos 1001, a non-coated pigment. The coated Kronos 1014, 1071 and 1080 show lower U_{max} values.
- In some cases remarkable differences in the PEMF parameters were observed for different anatase pigments. Despite the same composition, Kronos 1001 and Kronos 3000 differ in the parameter relations k_1/k_2 and U_1^0/U_2^0. Electron micrographs of Kronos 1001 and Kronos 3000 (Fig. 6) support the assumption that these differences are caused only by their different grain sizes. According to Fig. 6 Kronos 3000 consist of much larger particles than Kronos 1001. In comparison to Kronos 1001, the surface of the particles of Kronos 3000 is more rugged. So Kronos 3000 should contain more traps in the surface region than Kronos 1001 explaining the larger value of k_1/k_2.
- In the following we can show that coating of the rutile-type pigments causes the same changes in the PEMF parameters that it does in the case of anatase pigments:

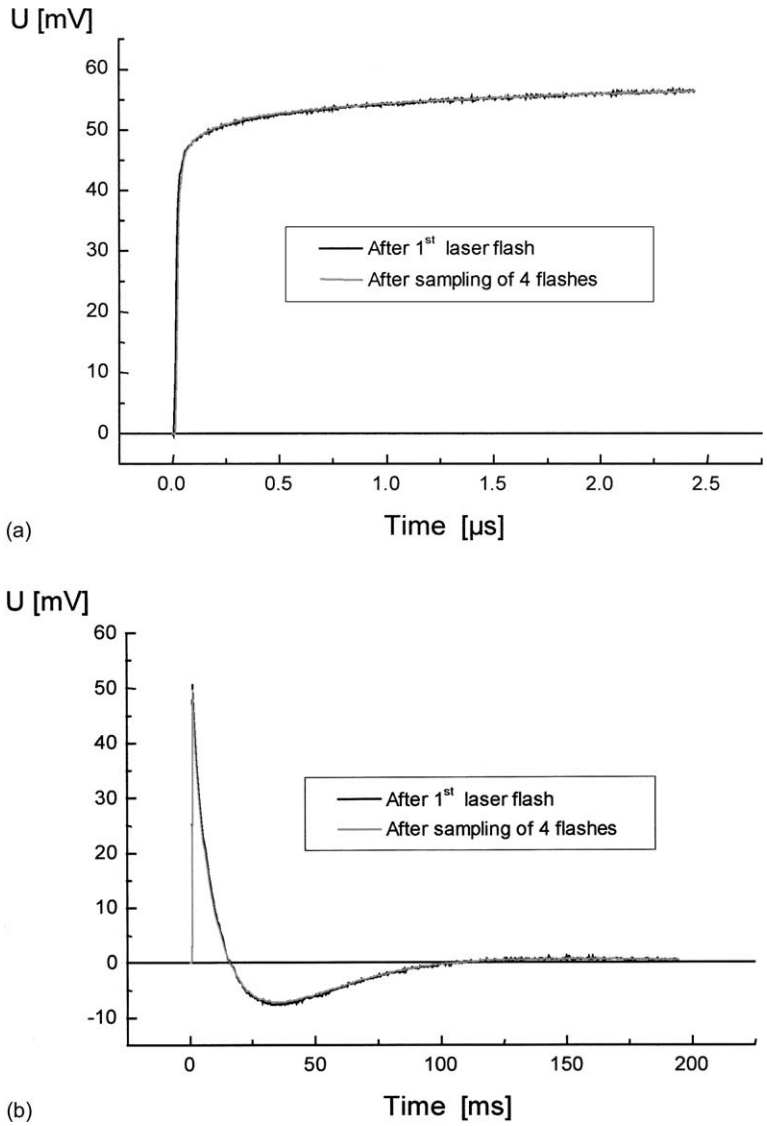

Fig. 4. PEMF signal of the uncoated anatase pigment Kronos 3000: (a) 0–2.5 μs; (b) 0–200 ms.

We can see that Kronos 3025, as an untreated rutile-type pigment, yields the highest U_{max}. In comparison to that, sample WJ 127/99, which is coated with a cross-linked silicon, shows a complicated PEMF signal with a smaller U_{max} value.

- Kronos 2400 also shows a very complex behaviour: The sign of U_{max} changes with increasing number of laser flashes; see Fig. 7 and Table 4. This indicate extremely deep traps in which the charges remain fixed for more than 120 s. As a result, internal potentials in sample are formed which change the direction of the charge carrier diffusion after the following flashes.
- Kronos 2044, 2056 and WJ 127/99 show very complex PEMF; Fig. 8. During the first 10 ms, signals with negative U_{max} and partially two intercepts with the 0-line were observed. Such signals indicate a surface treatment or/and heterogenic particles.
- A direct dependence of U_{max}, k_1 and k_2 on the content of coating is clear to see when considering the aluminium oxide coated rutile-types Kronos 2059, 2084, 2087 and 2400 of different coating thickness; Fig. 9. An exception is Kronos 2400 which cannot be explained by the available data.
- Considering the samples Kronos 2044, 2056, 2081 and 2220, which all have an aluminium oxide and silicon dioxide epitaxial coating of different thickness and at different concentration, a direct dependence of U_{max}, k_1 and k_2 on the content on titanium dioxide was found; Fig. 10. The ratio k_1/k_2 is nearly 1 which means that we found the same slope for both k values. This indicates that both coatings do level the behaviours of both subsurface and bulk. That means the added silicon and aluminium are situated both in the surface region and in the bulk. According to literature [15,16], Al^{3+} can occupy lattice places of

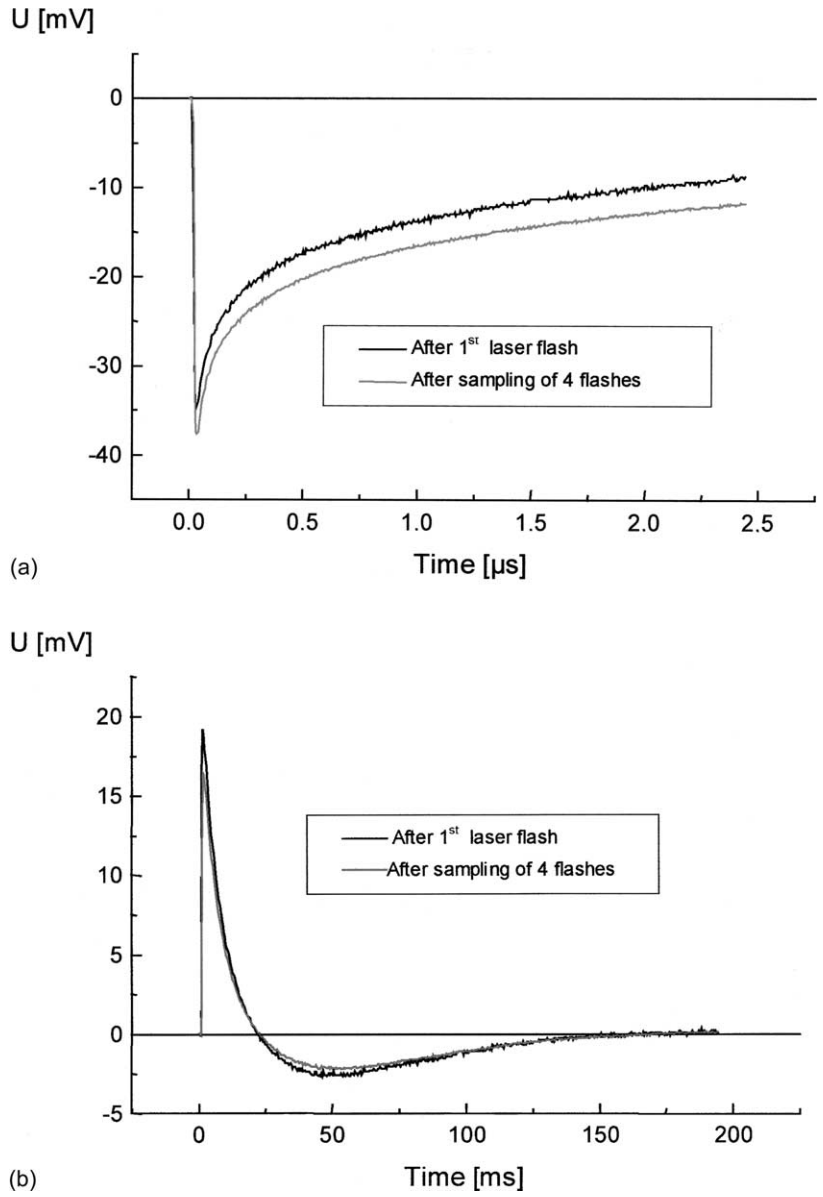

Fig. 5. PEMF signal of the uncoated rutile pigment Kronos 3025: (a) 0–2.5 μs; (b) 0–200 ms.

Table 4
Kinetic parameters of PEMF measurements of Kronos 2400 in PVB (nitrogen-laser excitation at 337 nm, about 2.7×10^{13} photons per flash, total absorption, time range 0–200 ms, sampling of four signals in series; time between two flashes: 120 s)

Flash	U_{max} (mV)	U_1 (mV)	U_2 (mV)	k_1 (s)[a]	k_2 (s)[a]
1	1.0	0.218	−0.122	32	32
2	0.6	0.151	−0.150	28	28
3	−0.9[a]				
4	−1.7	−0.003	0.001	206	59
5	−2.1	−0.003	0.001	188	37
6	−2.4	−0.003	0.001	162	32

[a] Signal has two intercepts with the 0-line and cannot be calculated using Eq. (1).

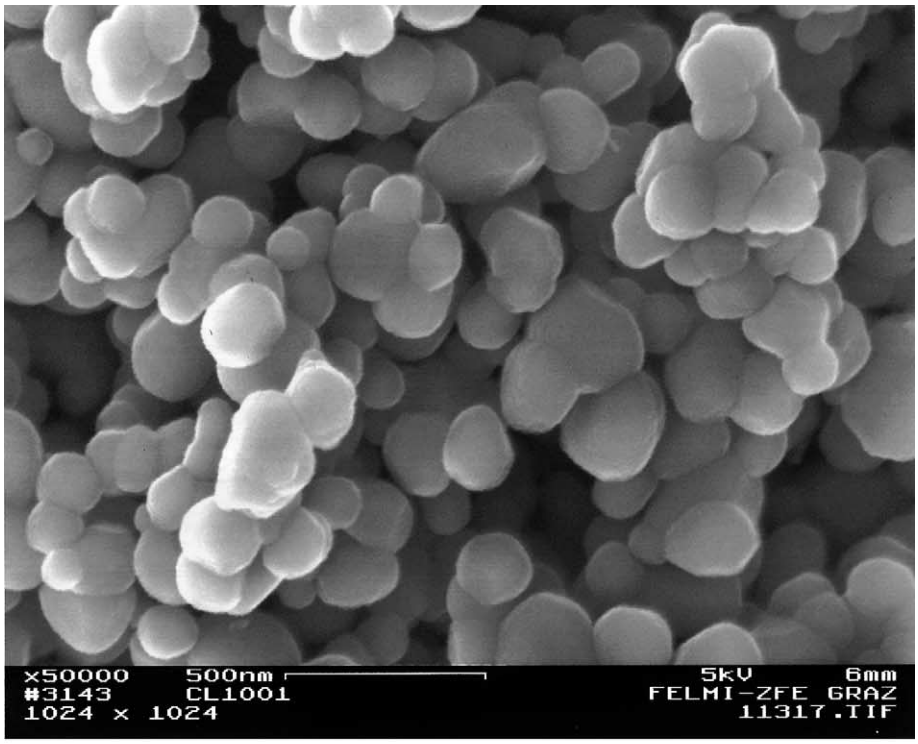

(a)

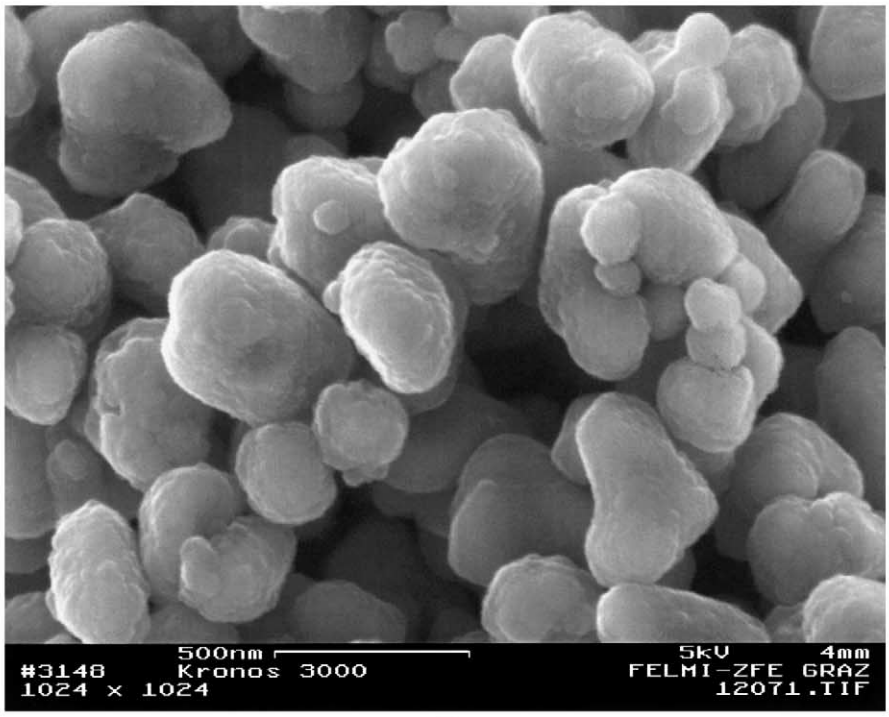

(b)

Fig. 6. Electron micrograph of the uncoated anatase pigments: Kronos 1001 (a) and Kronos 3000 (b).

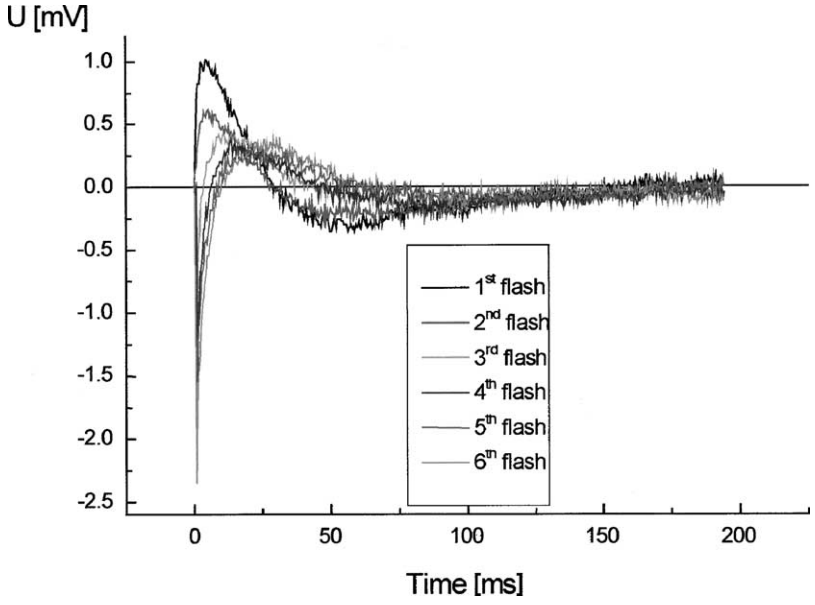

Fig. 7. PEMF signal of the rutile pigment Kronos 2400 (0–200 ms) as a function of the number of laser flashes.

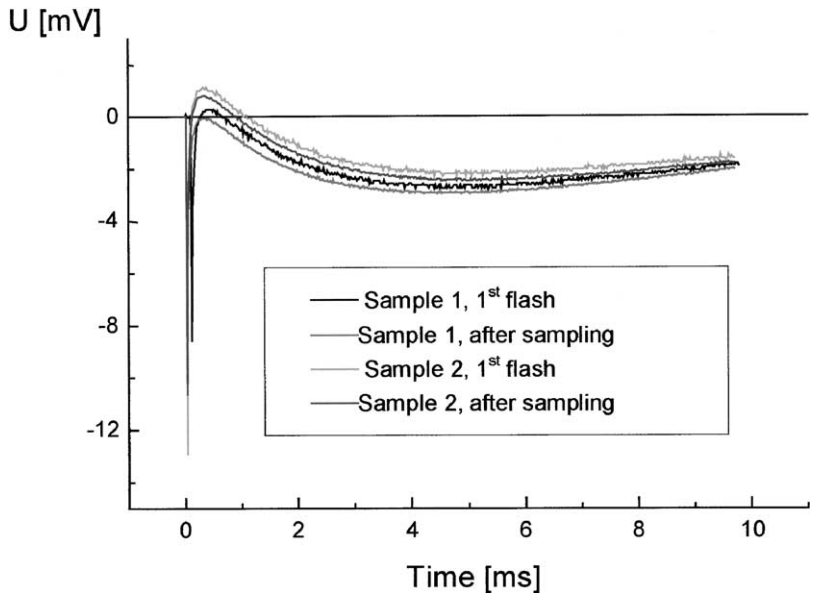

Fig. 8. PEMF signal of the Al_2O_3 and SiO_2 coated rutile pigment Kronos 2056.

Ti^{4+}. At high aluminium oxide concentrations the Al^{3+} ions are situated even on interstitial places. Moreover, aluminium oxide coats the surface of titanium dioxide pigments.

- An exception is the Kronos 2160 which is also described as both aluminium oxide and silicon oxide coated. Maybe the order of these coatings is exchanged. We assume that the aluminium oxide coating is the first and the silicon dioxide coating the second one, because the behaviour of Kronos 2160 would fit more to Kronos 2059 etc. In contrast the PEMF parameters of Kronos 2044 etc. indicate that the titanium dioxide was firstly coated with a silicon dioxide compound.

Based on the semi-quantitative weatherability in Table 1 and under the assumption that the weatherability of anatase-type pigments would be evaluated as 4 (=non-weatherable), we plotted U_{max} vs. these values; Fig. 11. We have found a qualitative dependence: The lower the (negative) U_{max}, the better the weatherability.

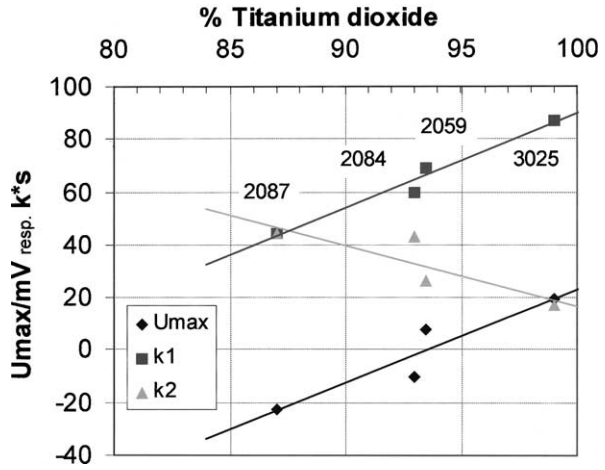

Fig. 9. Dependence of U_{max} resp. k on the content of titanium dioxide for aluminium coated rutiles.

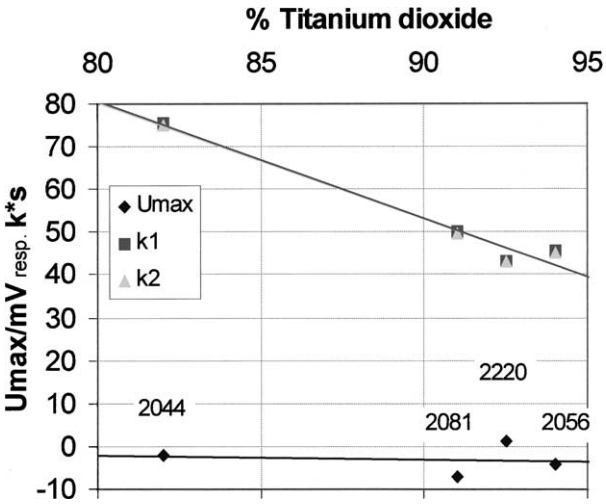

Fig. 10. Dependence of U_{max} resp. k on the content of titanium dioxide for aluminium + silicon (di)oxide coated rutiles.

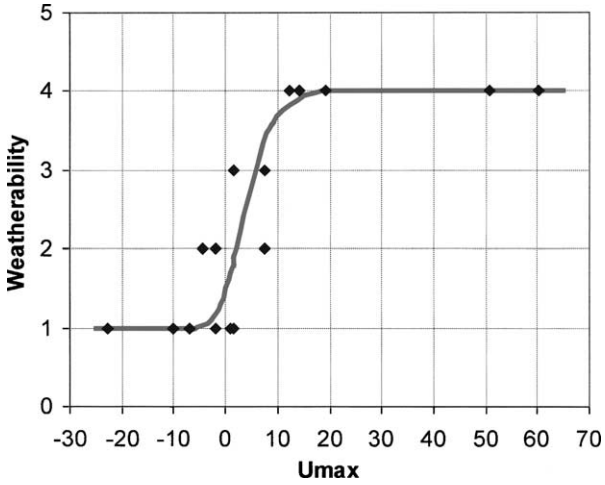

Fig. 11. Qualitative plot of U_{max} vs. weatherability (1: highest, 2: good, 3: yes, 4: no).

5. Conclusions

The results in Tables 2 and 3 show that the crystal structure (anatase or rutile) as well as type and concentration of the coating can influence the PEMF parameters of titanium dioxide pigments strongly. This means that the PEMF method is able to detect small differences in structure and composition of titanium dioxide pigments. According to the PEMF results, the investigated titanium dioxide pigments should have different photocatalytic activities.

Each coating of both anatase and rutile pigments results in a decrease of the maximum PEMF U_{max}. Moreover, in some cases the decay rate of PEMF does increase with increasing thickness of coating. Both results indicate an increase of the photostability of polymer compositions that contain such titanium dioxide pigments due to the coating. Last but not the least, PEMF parameters such as e.g. U_{max} give a quick indication of the weatherability of titanium dioxide pigments.

Acknowledgements

The authors wish to thank the Research Institute for Electron Microscopy (Graz, Austria) for the investigation using the electron microscopy.

References

[1] H. Chun, W. Yichong, T. Hongxiao, Chemosphere 41 (8) (2000) 1205.
[2] K. Wilke, H.D. Breuer, J. Inform. Rec. 24 (1998) 309;
C. Paulus, K. Wilke, H.D. Breuer, J. Inform. Rec. 24 (1998) 299.
[3] C. Morrison, J. Bandara, J. Kiuri, J. Adv. Oxid. Technol. 1 (2) (1996) 160.
[4] E. Pelizzetti, C. Minero, L. Tinucci, N. Serpone, Langmuir 9 (1993) 2995.
[5] D.W. Bahnemann, Israel J. Chem. 33 (1993) 115.
[6] C. Anton-Prinet, J.G. Mur, M. Gay, L. Adouin, J. Verdu, Polym. Degrad. Stabil. 60 (1998) 265.
[7] C. Anton-Prinet, J. Dubois, G. Mur, M. Gay, L. Audouin, J. Verdu, Polym. Degrad. Stabil. 60 (1998) 275.
[8] C. Anton-Prinet, J. Dubois, G. Mur, M. Gay, L. Audouin, J. Verdu, Polym. Degrad. Stabil. 60 (1998) 283.
[9] C. Decker, M. Balandier, Eur. Polym. J. 18 (1982) 1085.
[10] E.D. Owen, J.L. Williams, J. Polym. Sci. 12 (1974) 1933.
[11] M. Schiller, 3 Internationaler Kunststoff-Fenster-Kongress 2000, Berlin, February 1–2, 2000.
[12] G. Israel, F.W. Müller, C. Damm, J. Harenburg, J. Inform. Rec. 23 (1997) 559–584.
[13] F.W. Müller, C. Damm, G. Israel, J. Inform. Rec. 25 (2000) 533–552.
[14] Kronos TiO_2 Typen Anwendungsgebiete, Kronos Information 2.1, August 1998.
[15] U. Gesenhues, Solid State Ionics 101–103 (1997) 1171–1180.
[16] U. Gesenhues, J. Photochem. Photobiol. A 139 (2001) 243–251.